HHS Public Access

Author manuscript

Proc SPIE Int Soc Opt Eng. Author manuscript; available in PMC 2020 June 01.

Published in final edited form as:

Proc SPIE Int Soc Opt Eng. 2020 February ; 11222: . doi:10.1117/12.2546173.

Endosteal and periosteal blood flow quantified with dynamic contrast-enhanced fluorescence to guide open orthopaedic surgery

Shudong Jiang[a,*], **Jonathan T. Elliott**[a,b], **Jason R. Gunn**[a], **Cao Xu**[a], **Alberto J. Ruiz**[a], **Eric R. Henderson**[c], **Brian W. Pogue**[a], **I. Leah Gitajn**[c]

[a]Thayer School of Engineering, Dartmouth College, Hanover, NH

[b]Department of Surgery, Dartmouth-Hitchcock Medical Center, Hanover, NH

[c]Department of Orthopaedics, Dartmouth-Hitchcock Medical Center, Hanover, NH

Abstract

Due to the lack of objectively measurable or quantifiable methods to assess the bone perfusion, the success of removing devitalized bone is based almost entirely on surgeon's experience and varies widely across surgeons and centers. In this study, an indocyanine green (ICG)-based dynamic contrast-enhanced fluorescence imaging (DCE-FI) has been developed to objectively assess bone perfusion and guide surgical debridement. A porcine trauma model (n = 6 pigs × 2 legs) with up to 5 conditions of severity in loss of flow in each, was imaged by a commercial fluorescence imaging system. By applying the bone-specific hybrid plug-compartment (HyPC) kinetic model to four-minute video sequences, the perfusion-related metrics, such as peak intensity, total bone blood flow (TBBF) and endosteal bone blood flow to TBBF fraction (EFF) were calculated. The results shown that the combination of TBBF and EFF can effectively differentiate injured from normal bone with the accuracy, sensitivity and specificity of 89%, 88% and 90%, respectively. Our subsequent first in human bone blood flow imaging study confirmed DCE-FI can be successfully translated into human orthopaedic trauma patients.

Keywords

Dynamic contrast-enhanced fluorescence imaging; Indocyanine green; Orthopedic surgery; Boon blood flow; porcine trauma model

1. INTRODUCTION

Infection following bony fracture is highly prevalent and complicates the recovery of trauma patients, with an estimated annual cost of $35 billion in the US (https://stacks.cdc.gov/view/cdc/11550). Infection can be catastrophic, potentially causing prolonged morbidity, reduced function, permanent disability and and/or loss of limb. Failed treatment results in chronic bone infection requiring repeat surgical procedures in approximately 30% of

Shudong.jiang@dartmouth.edu.

patients. (1–4) Vascular perfusion is known to play a critical role in the health for trauma patients by delivering necessary oxygen, nutrients, antibiotics, and immune cells necessary to treat infection successfully(5–9). The management of trauma-related infection is therefore based on aggressive, thorough debridement of all poorly perfused bone and connective tissue, followed by fracture stabilization to prevent further injury. More extensive debridement is believed to improve treatment success; however, additional tissue loss requires increasingly complex reconstructive procedures to fill bone and connective tissue voids. At present there are no objective, intraoperative, and real-time techniques to assess bone perfusion and thoroughness of debridement. This unmet clinical need results in substantial practice variation and places patients at unnecessarily high risk for chronic infection and potentially avoidable surgical procedures.

Indocyanine green ICG fluorescence imaging has been used to assess tissue perfusion in vivo in real-time intra-operative arterial and lymphatic perfusion imaging,(10,11) osseous flap perfusion imaging(12). Compared to the conventional medical imaging modalities, such as CT or MRI, ICG fluorescence imaging is nonionizing, low-cost, and portable. Figure 1 shows the Schematic sketch of ICG fluorescence imaging. As shown in Fig.1, ICG fluorescence imaging utilizes intravenously injected ICG. ICG is a dye that absorbs near-infrared light in the wavelength range between 790 to 805 nm and has an emission at the peak of 835 nm. ICG is almost 98% plasma protein bound so that once it is taken up into the microcirculation, it remains within the lymphatic and circulatory vasculature. In addition, the ICG half-life is short making repeated measures possible, and it is indirectly activated, so that the dynamic fluorescence due to bone and tissue perfusion can be captured by a video rate imaging system. The video recording of fluorescence uptake and outflow allows collection of a rich dataset that not only includes a single measure of perfusion, (as reflected by the magnitude of ICG fluorescence), but also the slope of the fluorescence uptake, time to peak, time to plateau and outflow rate. ICG-based DCE-FI has enormous potential in translating fluorescence guided surgical principles to treatment of orthopedic conditions, such as infection and osteomyelitis, based on its safety profile, longstanding FDA approval status, history of success in operating room settings as well as its valuable imaging attributes including good signal to noise ratio, short half-life and ability to measure the inflow/outflow kinetics.

In this study, a porcine model has been used to demonstrate that quantitative indocyanine green (ICG)-based Dynamic Contrast Enhanced Fluorescence Imaging (DCE-FI) can assess bone perfusion in a measurable, reproducible and predictable way using.(13) Furthermore, we have initiated an Institutional Review Board (IRB)-approved protocol to perform similar imaging in human trauma patients with good success.

2. METHODS

2.1 Animal model

To demonstrate measurable, reproducible, and predictable differences in bone perfusion, quantitative ICG fluorescence imaging of a surgical porcine model was carried out in different conditions. The study protocol was approved by Dartmouth College's Institutional Animal Care and Use Committee (IACUC). The first 5 pigs (10 legs) explored five

conditions: (1) baseline; (2) two diaphyseal osteotomies, separating 1cm of tibia with circumferential soft tissue stripping (disrupting both periosteal and endosteal blood supply) (fracture model); (3) 2 cm circumferential soft tissue stripping (disrupting periosteal blood supply) from the proximal bone close to osteotomy (fracture model with periosteal stripping); (4) circumferential soft tissue stripping of the entire proximal bone segment (disrupting periosteal blood supply) (fracture model with additional periosteal stripping); and (5) circumferential soft tissue stripping of the entire bone (extensively disrupting periosteal blood supply) (fracture model with extensive periosteal stripping). In order to further demonstrate ICG fluorescence imaging could be used to assess not only the bone perfusion through periosteal but also endosteal blood supply, the sixth pig was designed to have three conditions (different than that of the study described above): (I) baseline, (II) ~2cm circumferential soft tissue stripping (disrupting periosteal blood supply), and (III) two diaphyseal osteotomies, separating this 2cm of tibia (disrupting both periosteal and endosteal blood supply).

2.2 ICG based Dynamic Contrast-Enhanced Fluorescence Imaging

For each condition shown in section 2.1, video image stream was captured by a fluorescence surgical imaging system (Pentero Zeiss and Spy Elite). Before imaging each condition, 0.1 mg/kg ICG was injected intravenously and the dynamic fluorescence change was captured by a fluorescence surgical imaging system for 4 minutes. A total of 20 minutes was allowed for elimination of residual ICG between each condition. As shown in Figure 2, there were five regions of interest (ROIs) studied: one ROI (t) is at the location of the osteotomy, two ROIs each at proximal (p1 & p2) and distal (d1 & d2), respectively. The length along each ROI is approximately 1 cm. For each of ROI, ICG intensity of all pixels inside of the ROI was averaged at each time point.

2.3 Bone-Specific Approach to Kinetic Modeling of Dynamic ICG Curves

A approaches(13) that has been used to assess cerebral blood flow using ICG curve shape has been modified to assess bone perfusion. As depicted in Figure 3, the dynamic tissue curves measured by the fluorescence imaging device represent a convolution between the arterial input function (AIF, $C_a(t)$) and the flow-scaled “impulse residue function (*R(t)* fraction of the dye at time, t, in the region of interrogation following an idealized ‘delta function’ bolus injection. Therefore, the dye concentration in the tissue is C(t) = Ca(t) * FR(t) by the convolution theorem first described by Meier et al(14), where C(t) is obtained from time series images of DCE-FI, Ca(t) is AIF and FR(t) is the flow scaled impulse residue function, (R(t) is mathematically defined as the fraction of remaining ICG in the region of interrogation at time, *t*, following an idealized bolus (temporal-delta function)). Therefore, any inferences made about properties of FR(t) on the basis of C(t), that don’t taken into account Ca(t), are prone to bias and variability. To exploit the difference in hemodynamics between the periosteal supply and the endosteal supply, a hybrid plug-compartment kinetic model for R(t) is defined based on the knowledge of the underlying bone physiology and with consideration paid to the limitations of the instrument’s temporal resolution. In this model, the bone cortex is supported by tow vascular ‘units’, periosteal vasculature and endosteal vasculature, where the first (periosteal) was as a plug and the second (endosteal) was as a simple two compartment tissue. In the first (capillary) phase, the

dye has not extravasated from the intravascular space, and variations in arrival time of dye are due completely to the distribution of transit times attributed to the variety of paths available in the “mesh” of capillaries. During the second (parenchyma) phase, there is exchange between the intravascular and extravascular extracellular space, modeled by an exponential function (first order rate equation). While this is an oversimplification of the physiology, it limits the degrees of freedom and avoids overfitting the measured data, while still providing quantitate variables with clinical relevance, such as endosteal blood flow (EBF) and periosteal blood flow (PBF), and their combinations of total bone blood flow (TBBF = PBF + EBF) and (d) endosteal flow fraction (EFF=EBF/TBBF).

3. RESULTS

Figure 4 shows the ICG fluorescence map overlay on the white light bone images as well as dynamic curves at the proximal and distal bones (green and blue Region of Interest (ROI) in middle bone models). As shown in Figure 4, the ICG intensity and dynamic changes are substantially different in different conditions and ROIs. Baseline conditions, without disruption of either periosteal or endosteal blood supplies demonstrated the highest ICG intensity. Similarly, the next highest intensity was noted in ROIs proximal and distal to the osteotomy, prior to any removal of periosteum (again, leaving endosteal and periosteal blood supply intact; however, bone disrupted by an osteotomy). As sequential soft tissue stripping was performed, sequentially removing periosteal blood supply, the ICG intensity decreased. The osteotomized fragment of bone, with both periosteal and endosteal blood supply disrupted, demonstrated the lowest ICG intensity and a flat dynamic curve. This experiment demonstrated that ICG intensity decreased in relation to progressive disruption in bony blood supply. Furthermore, with bone injury, the ICG fluorescent curve also changed shape in relation to progressive disruption in blood supply, which is reflective of the changing kinetics of blood flow into and out of the tissue in question.

As the summary data of the maximum intensity and TBBF of each ROIs at each condition for the 10 pig legs, ICG fluorescence and TBBF were the highest in bone with endosteal and periosteal blood supply intact; lowest in bone with both periosteal and endosteal blood supply disrupted; and in between of the above two conditions in bone with either periosteal/endosteal blood supply disrupted/endosteal blood supply intact. We also did a statistical analysis of the data that classified ROI to either injured or normal bone. P-values and AUC values of using each of I_{max}, TBBF and EFF for differentiating the injured from normal bone were 0.12 & 0.64, <0.001& 0.83, and <0.001 & 0.88, respectively. These values indicated the potential for using these variables as the indicators to diagnose bone health with high sensitivity and specificity, during the orthopedic surgery. Furthermore, we also adapted Support vector machine (SVM) classification to obtained the diagnostic performance of the combination of TBBF and EFF. Comparing to the signal variable of either I_{max}, or TBBF or EFF, combined TBBF and EFF obtained the best diagnostic performance of 89% accuracy, with the specificity of 88% and sensitivity of 90%, respectively.

To further demonstrate that ICG fluorescence imaging can assess the bone perfusion through either periosteal or endosteal blood supply, another porcine model study was conducted.

This study was designed to have three conditions (different than that of the study described above): (I) baseline, (II) ~2cm circumferential soft tissue stripping (disrupting periosteal blood supply), and (III) two diaphyseal osteotomies, separating this 2cm of tibia (disrupting both periosteal and endosteal blood supply). ICG fluorescence was imaged by SpyElite (Stryker, US). As the results, the maximum intensity decreased about 50% from baseline when soft tissue was stripped from the bone (disrupting the periosteal blood supply) and 98% from baseline when the bone was osteotomized (additionally disrupting the endosteal blood supply), as expected. This additional model, demonstrating measurable, reproducible and predictable differences in bone perfusion, and further validates the effectiveness of quantitative ICG fluorescence as a method of measuring bone perfusion.

4. CONCLUSIONS

This is the first study to apply ICG-based DCE-FI to assess bone perfusion in an orthopedic surgical setting. The results from porcine model suggest that ICG based DCE-FI has the potential to objectively/quantitatively measure bone perfusion and therefor inform intraoperatively to selective surgical debridement of the bone which profoundly affect the treatment of the complex traumatic injury as well as infection/osteomyelitis.

ACKNOWLEDGEMENTS

This work has been funded by a Dartmouth SYNERGY Grant (UL1TR001086), NIH/NCI K99CA190890 and NIH/NIBIB K23EB026507.

6. REFERENCES

1. Ehrlichman L, Rackard F, Sparks M, Harris M, and Gitajn I (2018) Factors associated with treatment failure of implant-related infections in fracture patients. in Orthopaedic Trauma Association Annual Meeting, Orlando, FL
2. Ovaska MT, Makinen TJ, Madanat R, Vahlberg T, Hirvensalo E, and Lindahl J (2013) Predictors of poor outcomes following deep infection after internal fixation of ankle fractures. Injury 44, 1002–1006 [PubMed: 23561581]
3. Rightmire E, Zurakowski D, and Vrahas M (2008) Acute infections after fracture repair: management with hardware in place. Clin Orthop Relat Res 466, 466–472 [PubMed: 18196433]
4. Reilly RM, Robertson T, O'Toole RV, and Manson TT (2016) Are antibiotic nails effective in the treatment of infected tibial fractures? Injury 47, 2809–2815 [PubMed: 27823759]
5. Jodal L, Nielsen OL, Afzelius P, Alstrup AKO, and Hansen SB (2017) Blood perfusion in osteomyelitis studied with [(15)O]water PET in a juvenile porcine model. EJNMMI Res 7, 4 [PubMed: 28091979]
6. Muller S, Gosau M, Strobel D, Gehmert S, Moralis A, Reichert TE, Prantl L, and Jung EM (2011) Assessment of bone microcirculation by contrast-enhanced ultrasound (CEUS) and [18F]-positron emission tomography/computed tomography in free osseous and osseocutaneus flaps for mandibular reconstruction: preliminary results. Clin Hemorheol Microcirc 49, 115–128 [PubMed: 22214683]
7. Stecker FF, Schierz JH, Opfermann T, Driesch D, Hofmann GO, Winkens T, and Freesmeyer M (2014) Early dynamic 18F-FDG PET/CT to diagnose chronic osteomyelitis following lower extremity fractures. A pilot study. Nuklearmedizin 53, 117–122 [PubMed: 23780221]
8. Freesmeyer M, Stecker FF, Schierz JH, Hofmann GO, and Winkens T (2014) First experience with early dynamic (18)F-NaF-PET/CT in patients with chronic osteomyelitis. Ann Nucl Med 28, 314–321 [PubMed: 24474597]
9. Marenzana M, and Arnett TR (2013) The Key Role of the Blood Supply to Bone. Bone Res 1, 203–215 [PubMed: 26273504]

10. Cahill RA, Ris F, and Mortensen NJ (2011) Near-infrared laparoscopy for real-time intra-operative arterial and lymphatic perfusion imaging. Colorectal Disease 13, 12–17 [PubMed: 22098511]
11. Reinhart MB, Huntington CR, Blair LJ, Heniford BT, and Augenstein VA (2016) Indocyanine Green: Historical Context, Current Applications, and Future Considerations. Surg Innov 23, 166–175 [PubMed: 26359355]
12. Valerio I, Green JM 3rd, Sacks JM, Thomas S, Sabino J, and Acarturk TO (2015) Vascularized osseous flaps and assessing their bipartate perfusion pattern via intraoperative fluorescence angiography. J Reconstr Microsurg 31, 45–53 [PubMed: 25469765]
13. Elliott JT, Jiang S, Pogue BW, and Gitajn IL (2019) Bone-specific kinetic model to quantify periosteal and endosteal blood flow using indocyanine green in fluorescence guided orthopedic surgery. J Biophotonics 4, 206–218
14. Meier P, and Zierler KL (1954) On the theory of the indicator-dilution method for measurement of blood flow and volume. J Appl Physiol 6, 731–744 [PubMed: 13174454]
15. Pine DJ, Weitz DA, Chaikin PM, and Herbolzheimer E (1988) Diffusing wave spectroscopy. Phys Rev Lett 60, 1134–1137 [PubMed: 10037950]

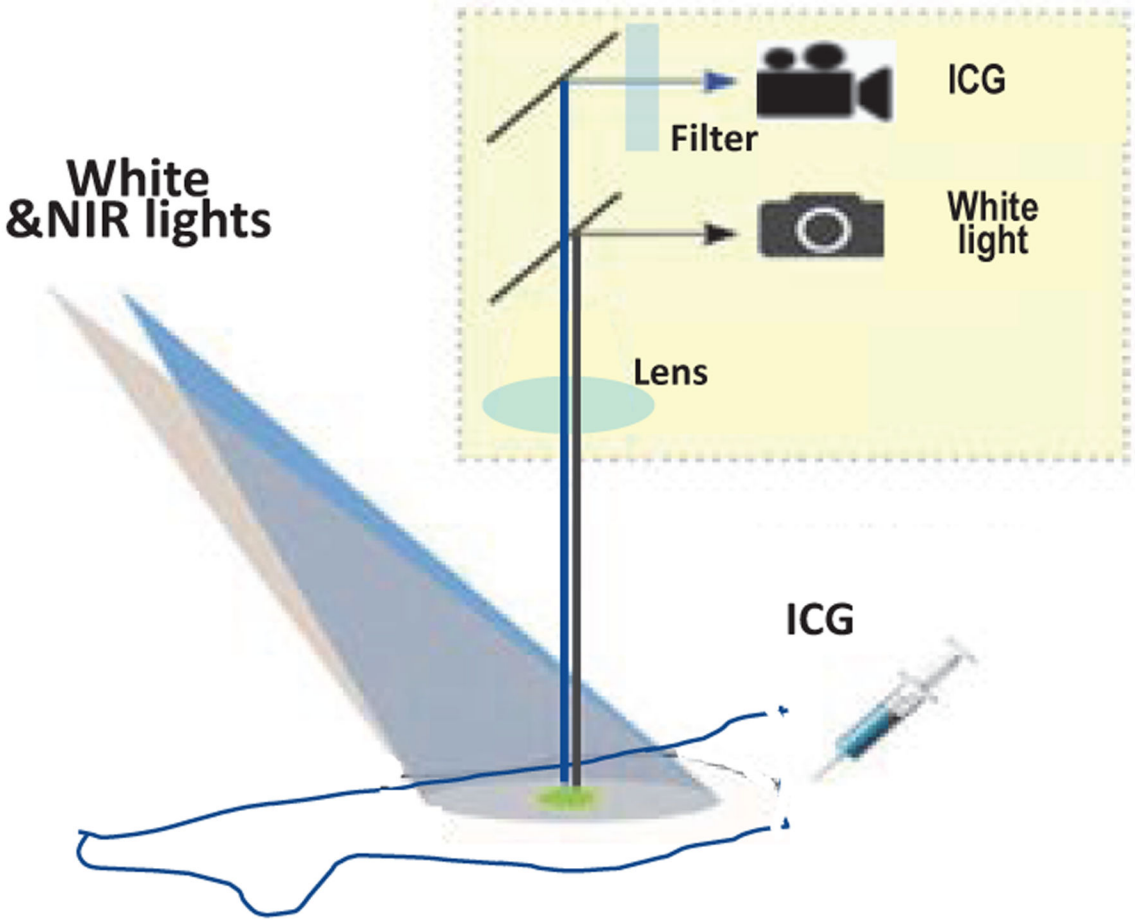

Figure 1:
Schematic sketch of ICG fluorescence imaging from filtered emission.

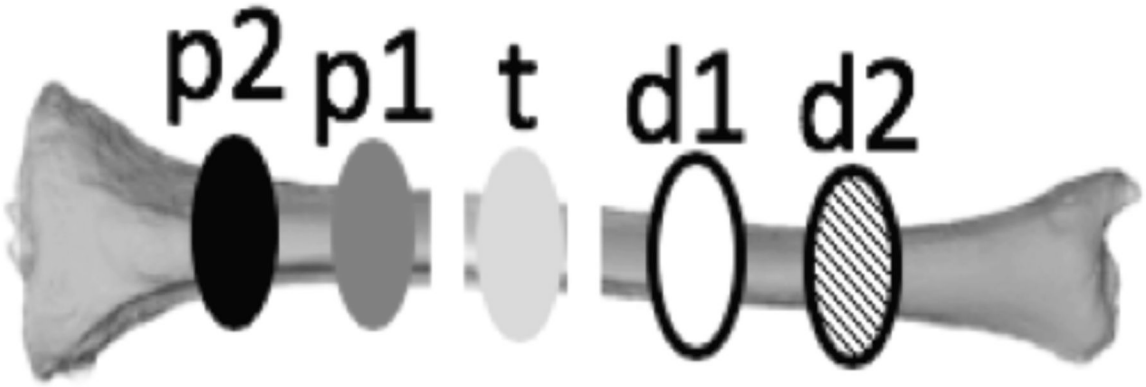

Figure 2:
Regions of interest (ROI). The area sizeof each ROI is about 10 mm length along the bone.P2 and P1 are the ROIs at proximal ends towards body, t is in the area that being osteotomized, and d1 and d2 are in the distal end of the tibia.

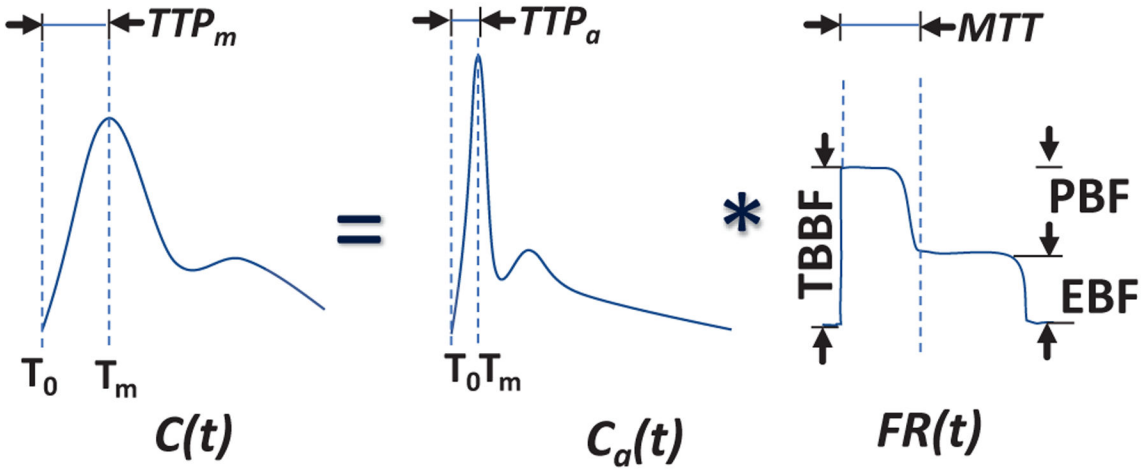

Figure 3:
Depiction of bone-specific kinetic model.

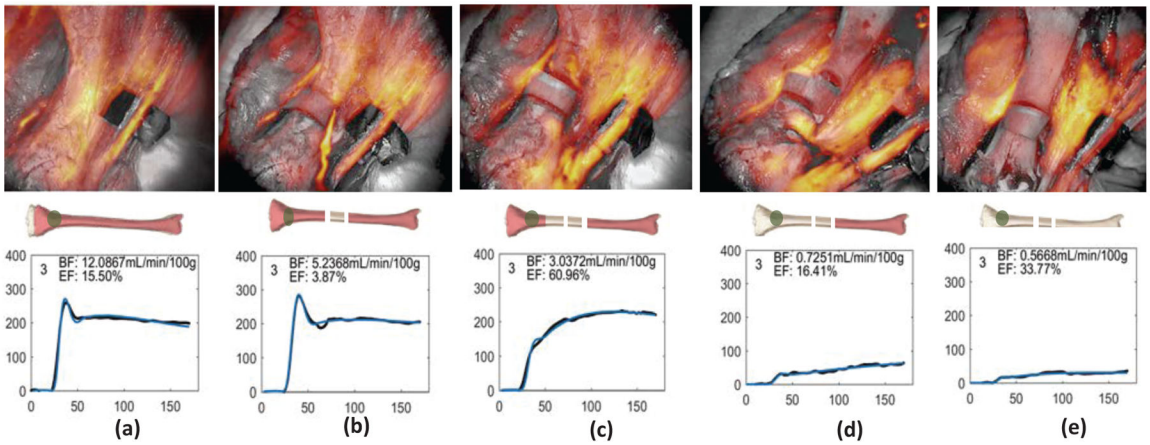

Figure 4:

ICG fluorescence map overlay on the white light bone images as well as temporal dynamic curves of the ICG kinetics in the ROI. (a) baseline, (b) after double diaphyseal osteotomies, (c) half circumferential soft tissue stripping from the proximal bone close to the previous cut, (d) full circumferential soft tissue stripping from the proximal end, and (e) all circumferential soft tissue stripping to disrupt both periosteal and endosteal blood supply from entire tibia.